Tokyo Climate Center, Japan Meteorological Agency

TCC News

No. 32 Spring 2013

Contents Page

El Niño Outlook (April – October 2013)

ENSO-neutral conditions are likely to continue during the Northern Hemisphere spring and summer.

El Niño/La Niña

In March 2013, the NINO.3 sea surface temperature (SST) was near normal with a deviation of +0.1°C. No significant SST anomalies were observed in the equatorial Pacific (Figures 1 and 3 (a)), while subsurface temperatures were above normal in the western equatorial Pacific (Figures 2 and 3 (b)). In the atmosphere, convective activity was greater than normal over the western equatorial Pacific. As these oceanic and atmospheric conditions were not characteristic of El Niño/La Niña events, it is considered that ENSO-neutral conditions continued in the equatorial Pacific area.

According to JMA's El Niño prediction model, the NINO.3 SST will be mostly near normal during the forecast period (Figure 4). In March, warm subsurface waters were seen in the western equatorial Pacific, while no significant temperature anomalies were observed in the central and eastern parts. These subsurface ocean conditions are not likely to significantly affect SSTs in the eastern part in the months ahead. In conclusion, it is likely that ENSO-neutral conditions will continue during the Northern Hemisphere spring and summer.

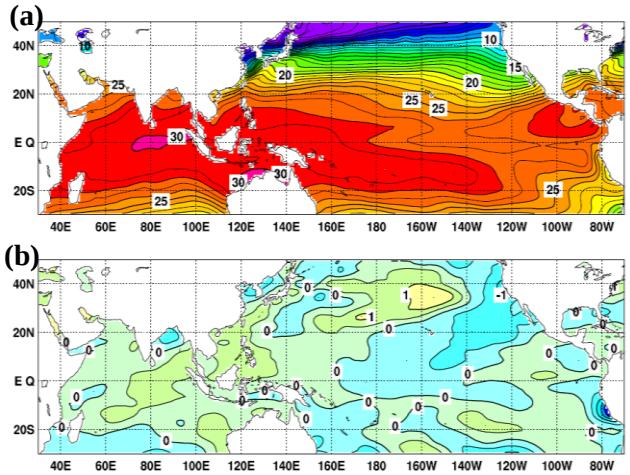

Figure 1 Monthly mean (a) sea surface temperatures (SSTs) and (b) SST anomalies in the Indian and Pacific Ocean areas for March 2013
The contour intervals are 1˚C in (a) and 0.5˚C in (b). The base period for the normal is 1981 – 2010.

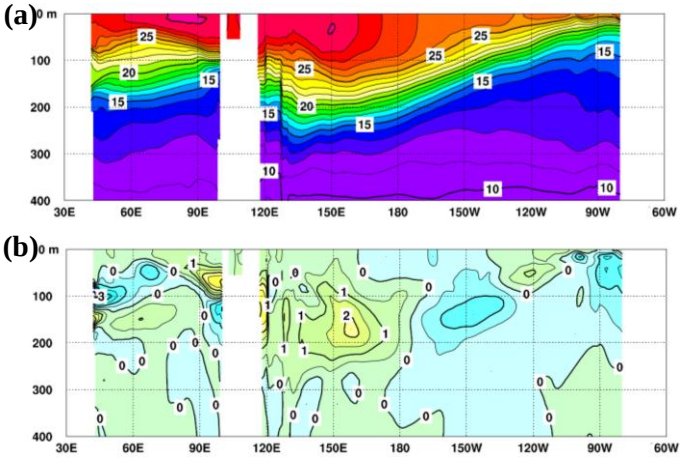

Figure 2 Monthly mean depth-longitude cross sections of (a) temperature and (b) temperature anomalies in the equatorial Indian and Pacific Ocean areas for March 2013
The contour intervals are 1˚C in (a) and 0.5˚C in (b). The base period for the normal is 1981 – 2010.

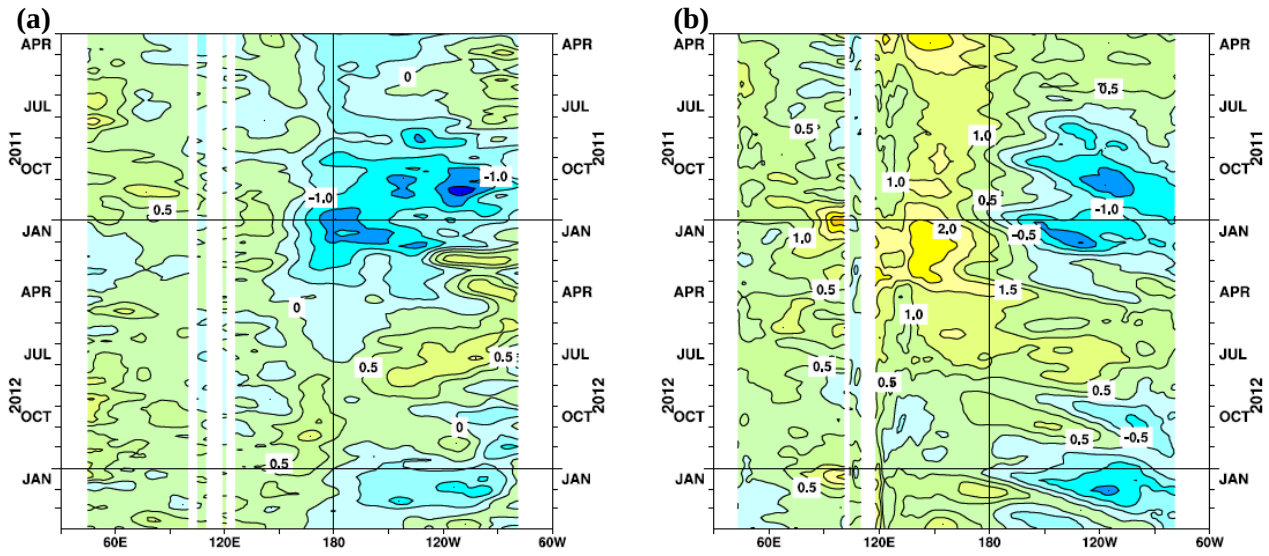

Figure 3 Time-longitude cross sections of (a) SST and (b) ocean heat content (OHC) anomalies along the equator in the Indian and Pacific Ocean areas

OHCs are defined here as vertical averaged temperatures in the top 300 m. The base period for the normal is 1981 – 2010.

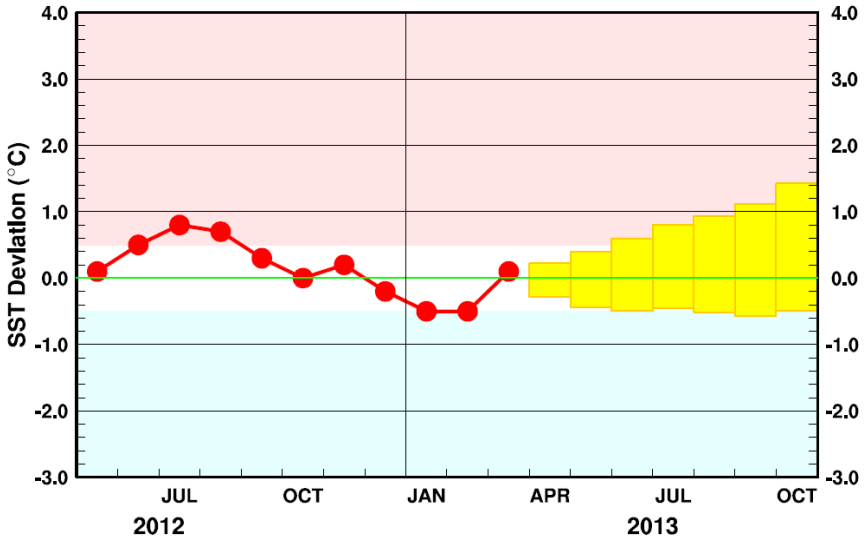

Figure 4 Outlook of NINO.3 SST deviation produced by the El Niño prediction model

This figure shows a time series of monthly NINO.3 SST deviations. The thick line with closed circles shows observed SST deviations, and the boxes show the values produced for the next six months by the El Niño prediction model. Each box denotes the range into which the SST deviation is expected to fall with a probability of 70%.

Western Pacific and Indian Ocean

The area-averaged SST in the tropical western Pacific (NINO.WEST) region was near normal in March, and is likely to remain mostly near normal during the Northern Hemisphere spring and summer.

The area-averaged SST in the tropical Indian Ocean (IOBW) region was above normal in March, and is likely to move closer to normal in the months ahead and near or below normal during the Northern Hemisphere summer.

(Ichiro Ishikawa, Climate Prediction Division)

* The SST normal for the NINO.3 region (5°S – 5°N, 150°W – 90°W) is defined as the monthly average over a sliding 30-year period (1983 – 2012 for 2013).
* The SST normals for the NINO.WEST region (Eq. – 15°N, 130°E – 150°E) and the IOBW region (20°S – 20°N, 40°E – 100°E) are defined as linear extrapolations with respect to a sliding 30-year period in order to remove the effects of significant long-term warming trends observed in these regions.

JMA's Seasonal Numerical Ensemble Prediction for Summer 2013

Based on JMA's seasonal ensemble prediction system, active convection is expected from the eastern part of the Indian Ocean to the western tropical Pacific, while inactive convection is expected in the western part of the Indian Ocean and the eastern part of the Pacific. In association with active convection over the tropical Indian Ocean, the North Pacific High is expected to be more enhanced than climatological values would suggest.

1. Introduction

This article outlines JMA's dynamical seasonal ensemble prediction for summer 2013 (June – August, referred to as JJA), which was used as a basis for the Agency's operational warm-season outlook issued on 25 April, 2013. The outlook detailed here is based on the seasonal ensemble prediction system of the Coupled atmosphere-ocean General Circulation Model (CGCM). See the column below for system details.

Section 2 outlines global SST anomaly predictions, and Section 3 describes the associated circulation fields expected over the tropics and sub-tropics. Finally, the circulation fields predicted for the mid- and high latitudes of the Northern Hemisphere are discussed in Section 4.

2. SST anomalies (Figure 5)

Figure 5 shows predicted SSTs and related anomalies for JJA. As values from central to eastern parts of the equatorial Pacific are not significant, ENSO-neutral (neither El Niño nor La Niña) conditions are expected throughout the period. In the western tropical Pacific, SST anomalies are also not significant, but are slightly above normal. In the Indian Ocean, SSTs are expected to be near normal on average but slightly below normal in the western part.

3. Prediction for the tropics and sub-tropics (Figure 6)

Figure 6 (a) shows predicted precipitation and related anomalies for JJA. In association with the contrast of SST anomalies between the Indian Ocean and the western tropical Pacific, precipitation amounts are expected to be above normal from Southeast Asia to the western tropical Pacific and below normal in the western part of the Indian Ocean.

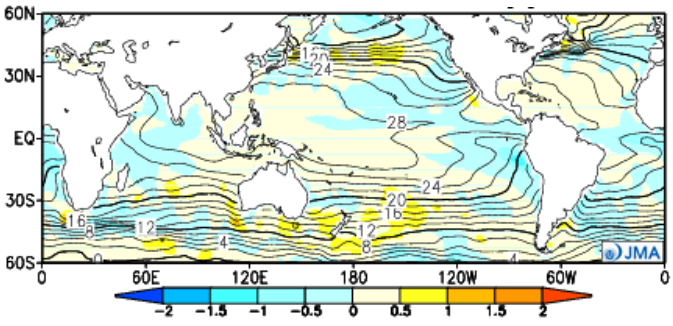

Figure 5 Predicted SSTs (contours) and SST anomalies (shading) for June – August 2013 (ensemble mean of 51 members)

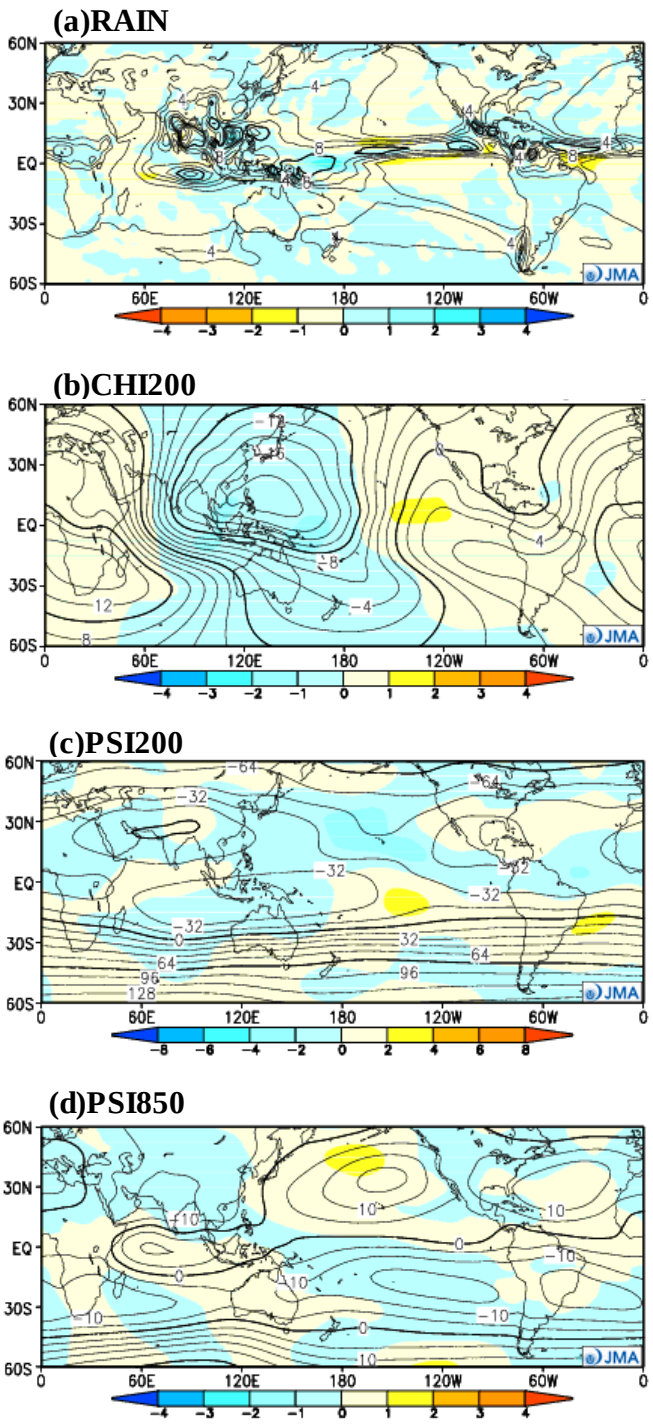

Figure 6 Predicted atmospheric fields from 60°N – 60°S for June – August 2013 (ensemble mean of 51 members)

(a) Precipitation (contours) and anomaly (shading). The contour interval is 2 mm/day.

(b) Velocity potential at 200 hPa (contours) and anomaly (shading). The contour interval is 2×10^6 m^2/s.

(c) Stream function at 200 hPa (contours) and anomaly (shading). The contour interval is 16×10^6 m^2/s.

(d) Stream function at 850 hPa (contours) and anomaly (shading). The contour interval is 5×10^6 m^2/s.

Velocity potential in the upper troposphere (200 hPa) (Figure 6 (b)) is expected to be negative (i.e., more divergent) from the eastern part of the Indian Ocean to the western tropical Pacific, reflecting active convection in these regions. Conversely, positive (i.e., more convergent) anomalies are expected both in the western part of the Indian Ocean and in the eastern tropical Pacific, reflecting inactive convection. The stream function at 200 hPa (Figure 6 (c)) is expected to be negative (i.e., cyclonic) around East Asia.

The stream function at 850 hPa (Figure 6 (d)) is expected to be negative (i.e., anti-cyclonic) from Southeast Asia to the western tropical Pacific, suggesting an enhanced monsoon trough. Conversely, positive (i.e., anti-cyclonic) anomalies are expected over the north Pacific, suggesting an enhanced North Pacific High.

4. Prediction for the mid- and high latitudes of the Northern Hemisphere (Figure 7)

Geopotential height anomalies at 500 hPa (Figure 7 (a)) are expected to be positive over most of the Northern Hemisphere. However, negative anomalies are expected in some parts around East Asia, which may be related to the enhanced monsoon trough seen in the stream function at 850 hPa.

Positive anomalies of sea level pressure (Figure 7 (b)) are expected in most regions of the North Pacific, suggesting an enhanced North Pacific High. These anomalies are consistent with the positive anomalies of the stream function at 850 hPa.

(Masayuki Hirai, Climate Prediction Division)

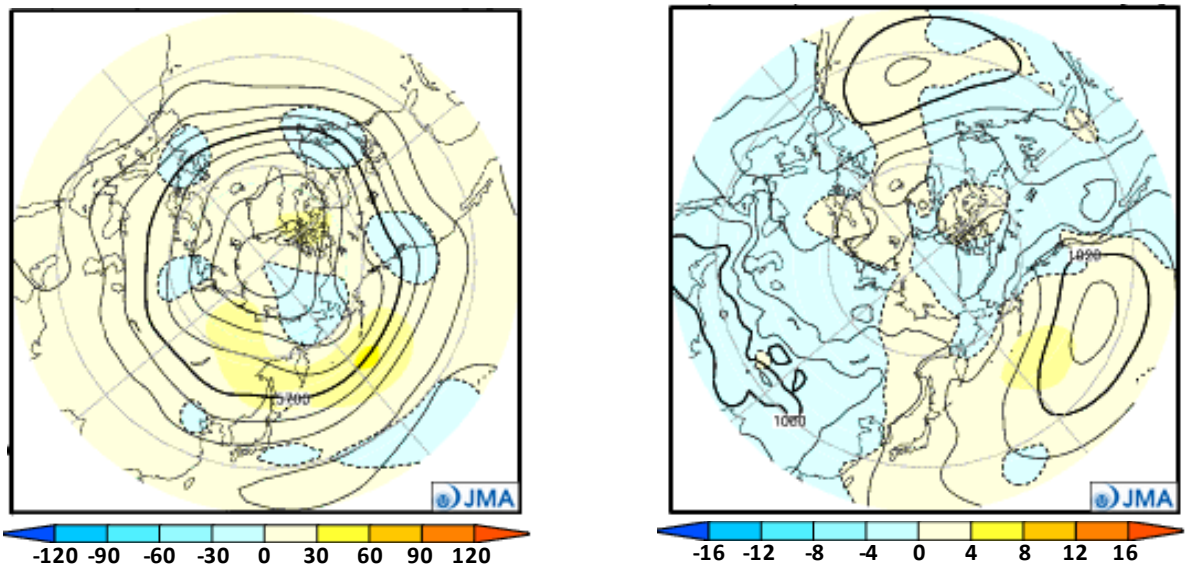

Figures 7 Predicted atmospheric fields from 20°N – 90°N for June – August 2013 (ensemble mean of 51 members)
(a) Geopotential height at 500 hPa (contours) and anomaly (shading). The contour interval is 60 m.
(b) Sea level pressure (contours) and anomaly (shading). The contour interval is 4 hPa.

JMA's Seasonal Ensemble Prediction System

JMA operates a seasonal Ensemble Prediction System (EPS) using the Coupled atmosphere-ocean General Circulation Model (CGCM) to make seasonal predictions beyond a one-month time range. The EPS produces perturbed initial conditions by means of a combination of the initial perturbation method and the lagged average forecasting (LAF) method. The prediction is made using 51 members from the latest six initial dates (nine members are run every five days). Details of the prediction system and verification maps based on 30-year hindcast experiments (1979 – 2008) are available at http://ds.data.jma.go.jp/tcc/tcc/products/model/.

Warm Season Outlook for Summer 2013 in Japan

In summer 2013, mean temperatures are likely to be near or above normal, both with a 40% probability, in northern, eastern and western Japan. Warm-season precipitation amounts are expected to be near or above normal, both with a 40% probability, in Okinawa/Amami.

1. Outlook summary

JMA issued its outlook for the coming summer over Japan in February and updated it in March and April. In summer 2013, mean temperatures are likely to be near or above normal, both with a 40% probability, in northern, eastern and western Japan. Summer total precipitation amounts are expected to be near or above normal, both with a 40% probability, in Okinawa/Amami (Figures 8 and 9). Rainy season (Baiu) precipitation amounts are unlikely to exhibit particular characteristics in any region.

2. Outlook background

JMA's coupled global circulation model predicts that ENSO-neutral conditions will continue during the spring and summer of 2013.

SSTs are predicted to be higher than normal from the eastern Indian Ocean to the western tropical Pacific in summer and lower than normal in the western tropical Indian Ocean and the eastern equatorial Pacific.

In association with these SST anomalies, atmospheric convection is predicted to be more active than normal from the eastern Indian Ocean to the western tropical Pacific and less active than normal over the western tropical Indian Ocean and the eastern tropical Pacific. The Tibetan high is expected to be stronger than normal due to the active convection from the eastern Indian Ocean to the western tropical Pacific. As a result, the subtropical jet, which flows along the northern edge of the Tibetan high, is expected to shift northward of its normal position.

The tropospheric thickness temperature averaged over the mid-latitudes of the Northern Hemisphere (30°N – 50°N), which shows a correlation with temperatures over Japan, is predicted to be slightly above normal.

In terms of the characteristics of atmospheric circulation around Japan, the northwestern part of the North Pacific High is expected to be stronger than normal in association with the northward shift of the subtropical jet from its normal position. Northern, eastern and western Japan are expected to experience above or near normal temperatures due to coverage by the North Pacific High. The Okinawa/Amami region is expected to be influenced by moist southerly flows occurring with a greater frequency than normal around the western edge of the North Pacific High.

(Takafumi Umeda, Climate Prediction Division)

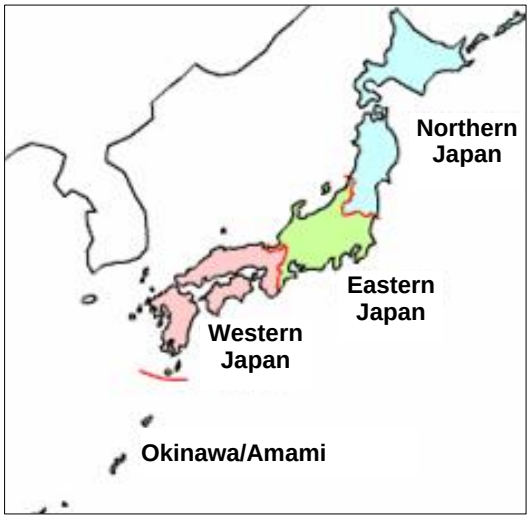

Category	−	0	+
Northern Japan	20	40	40
Eastern Japan	20	40	40
Western Japan	20	40	40
Okinawa and Amami	30	40	30

(Category −: below normal, 0 : normal, + : above normal, Unit: %)

Figure 8 Outlook for summer 2013 temperature probability in Japan

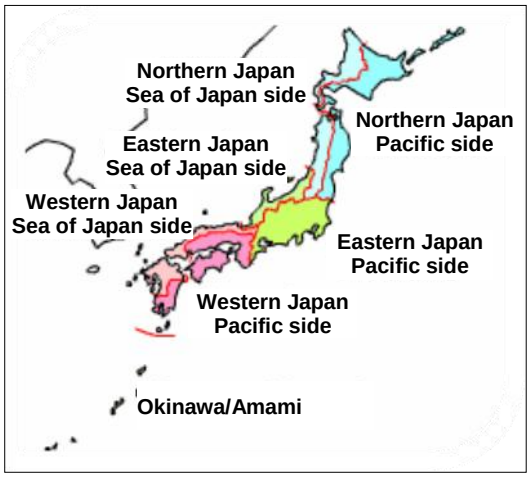

Category		−	0	+
Northern Japan	Sea of Japan side	40	30	30
	Pacific side	40	30	30
Eastern Japan	Sea of Japan side	40	30	30
	Pacific side	40	30	30
Western Japan	Sea of Japan side	30	40	30
	Pacific side	30	40	30
Okinawa and Amami		20	40	40

(Category −: below normal, 0 : normal, + : above normal, Unit: %)

Figure 9 Outlook for summer 2013 precipitation probability in Japan

Summary of the 2012/2013 Asian Winter Monsoon

Northern East Asia, especially the area from eastern Mongolia to northeastern China, experienced cold winter conditions in 2012/2013 as it did in winter 2011/2012. This report summarizes the characteristics of the surface climate and atmospheric/oceanographic considerations related to the Asian winter monsoon for 2012/2013 with focus on the cold conditions observed.

Note: JRA/JCDAS (Onogi et al. 2007) atmospheric circulation data and COBE-SST (JMA 2006) sea surface temperature (SST)/sea ice concentration data were used for this investigation. The outgoing longwave radiation (OLR) data referenced to infer tropical convective activity were originally provided by NOAA. The base period for the normal is 1981 – 2010. The term "anomaly" as used in this report refers to deviation from the normal.

1. Surface climate conditions

In winter 2012/2013, temperatures were lower than normal in northern Asian countries and higher than normal in southern Asian countries and eastern Siberia (Figure 10). Temperatures were 6°C below normal from the southern part of central Siberia to northeastern Kazakhstan in December and around the northern part of eastern Siberia in February.

Figure 11 shows extreme climate events that occurred from December 2012 to February 2013. In December, extremely high temperatures were observed from the Philippines to southern India, and extremely low temperatures were observed from western Japan to Kazakhstan. Figure 12 shows daily temperatures at Shenyang in China and Ulaanbaatar in Mongolia. Daily mean temperatures were below normal throughout most of the winter at Shenyang and during the whole winter except the second half of January at Ulaanbaatar. In January and February, extremely high temperatures were observed in southern Asian countries.

In December, it was reported that a cold wave caused more than 130 fatalities in India and more than 70 in Bangladesh (EM-DAT). The Philippine Government also reported that Typhoon Bopha caused more than 1,000 fatalities in the country in early December 2012.

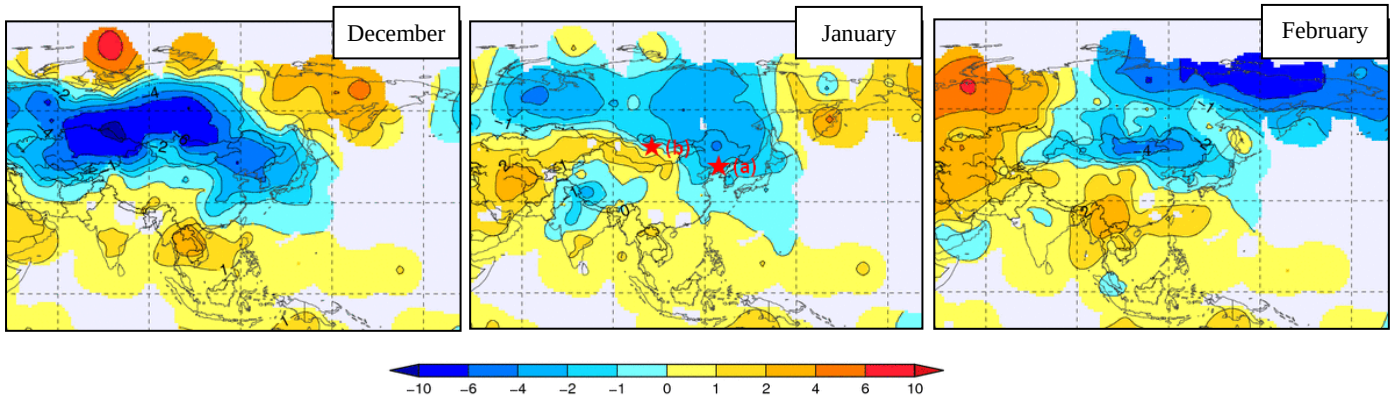

Figure 10 Monthly mean temperature anomalies from December 2012 to February 2013
Anomalies are deviations from the normal (i.e., the 1981 – 2010 average). Daily temperature data for (a) Shenyang (China) and (b) Ulaanbaatar (Mongolia) on the maps are shown in Figure 12.

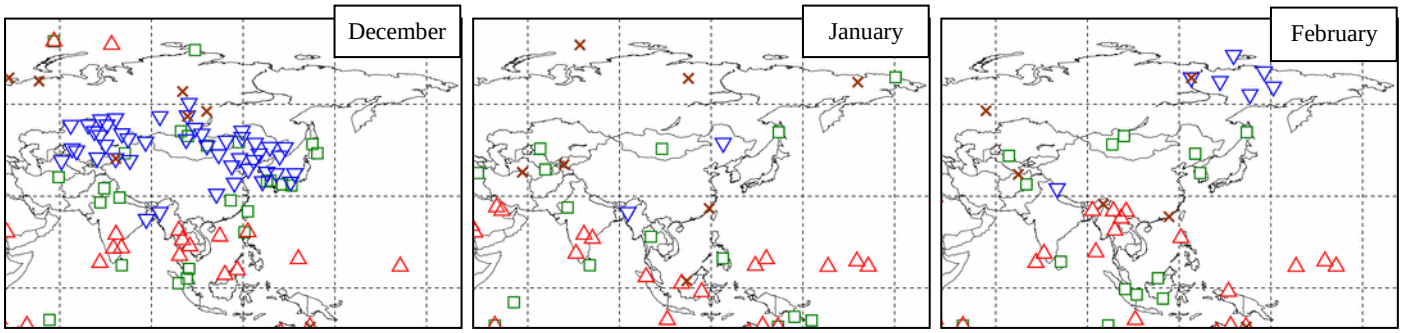

Figure 11 Extreme climate events from December 2012 to February 2013
△ Extremely high temperature (ΔT/SD ≥ 1.83) □ Extremely heavy precipitation (Rd = 6)
▽ Extremely low temperature (ΔT/SD ≤ -1.83) × Extremely light precipitation (Rd = 0)
ΔT, SD and Rd indicate temperature anomaly, standard deviation and quintile, respectively.

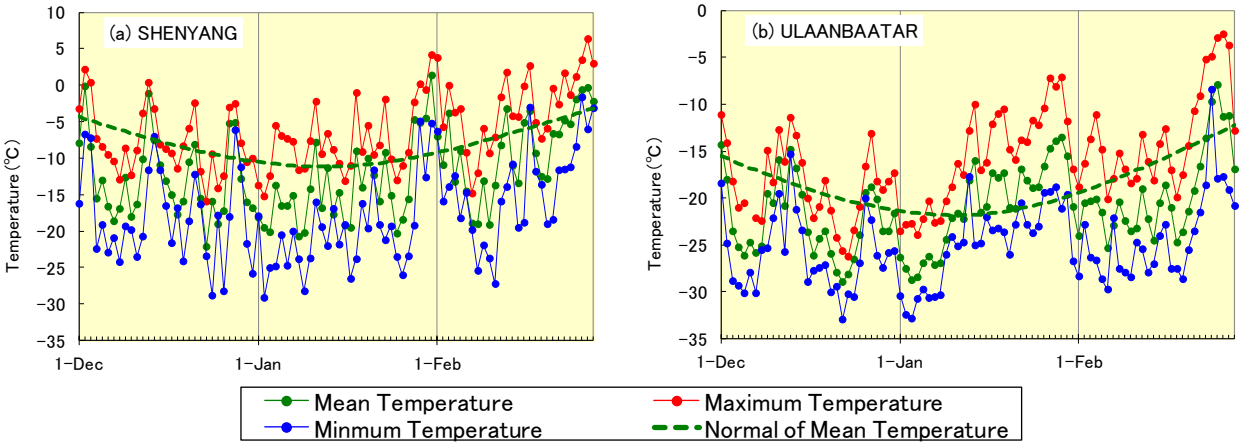

Figure 12 Daily maximum, mean and minimum temperatures (°C) at Shenyang in China and Ulaanbaatar in Mongolia from December 2012 to February 2013 (based on SYNOP reports)

2. Characteristic atmospheric circulation causing the cold winter conditions

In winter 2012/2013, sea surface temperatures (SSTs) in the central and eastern equatorial Pacific were below normal, but no La Niña event occurred (Figure 13). SST anomalies indicated warm conditions in the Indian Ocean and the western tropical Pacific, and were significantly above normal in the eastern Indian Ocean and around the Maritime Continent. In line with the enhanced convective activity observed around the eastern Indian Ocean (Figure 14), divergence anomalies were seen there in the upper troposphere (Figure 15 (a)). Wave trains were observed along the Asian jet stream with upper-level anticyclonic and cyclonic circulation anomalies around southern China and over the area to the east of Japan, respectively (Figure 15 (b)).

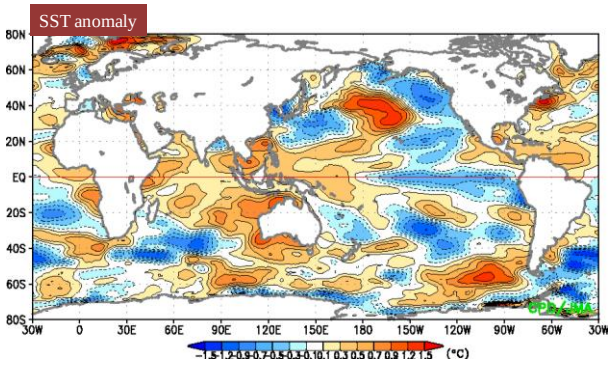

Figure 13 Three-month mean sea surface temperature (SST) anomalies for December 2012 – February 2013

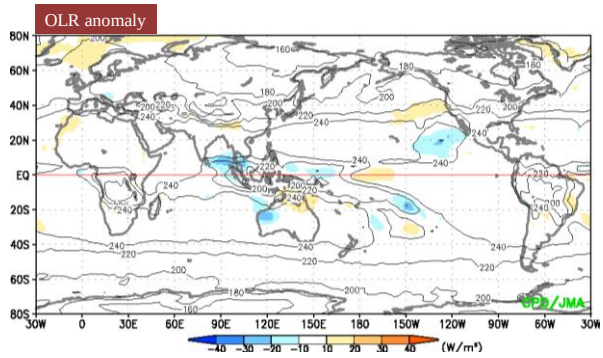

Figure 14 Three-month mean outgoing longwave radiation (OLR) anomalies for December 2012 – February 2013

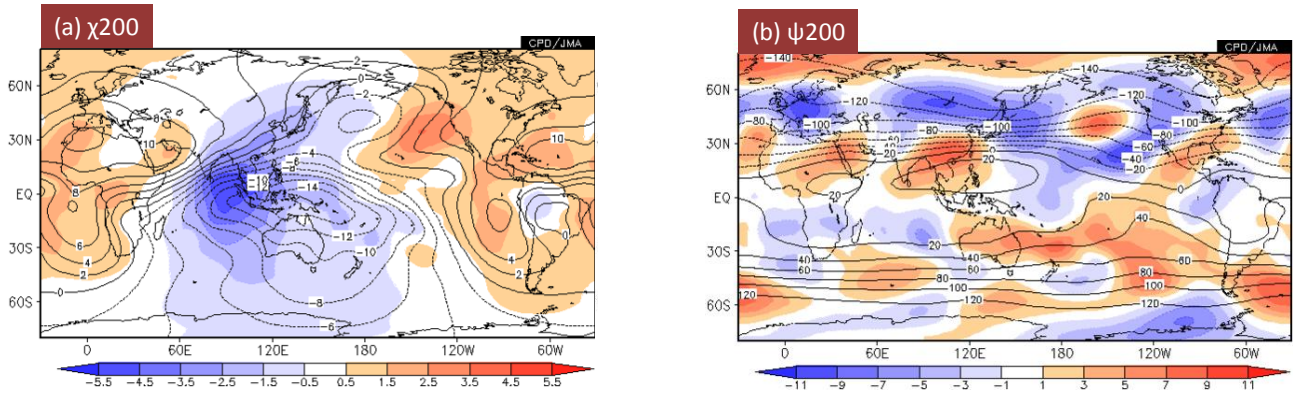

Figure 15 Three-month mean 200-hPa velocity potential and stream function for December 2012 – February 2013
(a) The contours indicate velocity potential at intervals of 2×10^6 m^2/s, and the shading shows related anomalies.
(b) The contours indicate stream function at intervals of 20×10^6 m^2/s, and the shading shows related anomalies.

In the Northern Hemisphere, atmospheric circulation observed during winter featured annular patterns with positive anomalies over the Arctic region and negative anomalies over the mid-latitudes in the troposphere and the stratosphere, indicating negative Arctic Oscillation (AO)-like conditions (Figures 16 (a) – (d)). In association, the polar-front jet stream was generally shifted southward of its normal position over the North Atlantic and Eurasia (Figure 16 (e)), and temperatures in the lower troposphere were below normal over most parts of the Eurasian mid- and high latitudes (Figure 16 (f)).

On the 310-K isentropic surface approximately corresponding to 300-hPa geopotential height in the high latitudes (Figure 17), negative potential vorticity (PV) anomalies were seen over eastern Siberia and the area to the north of Europe, indicating frequent development of blocking highs. Positive PV anomalies were observed from Mongolia to northern Japan in association with blocking flows, indicating frequent movement of split polar vortices with cold air masses toward northern East Asia.

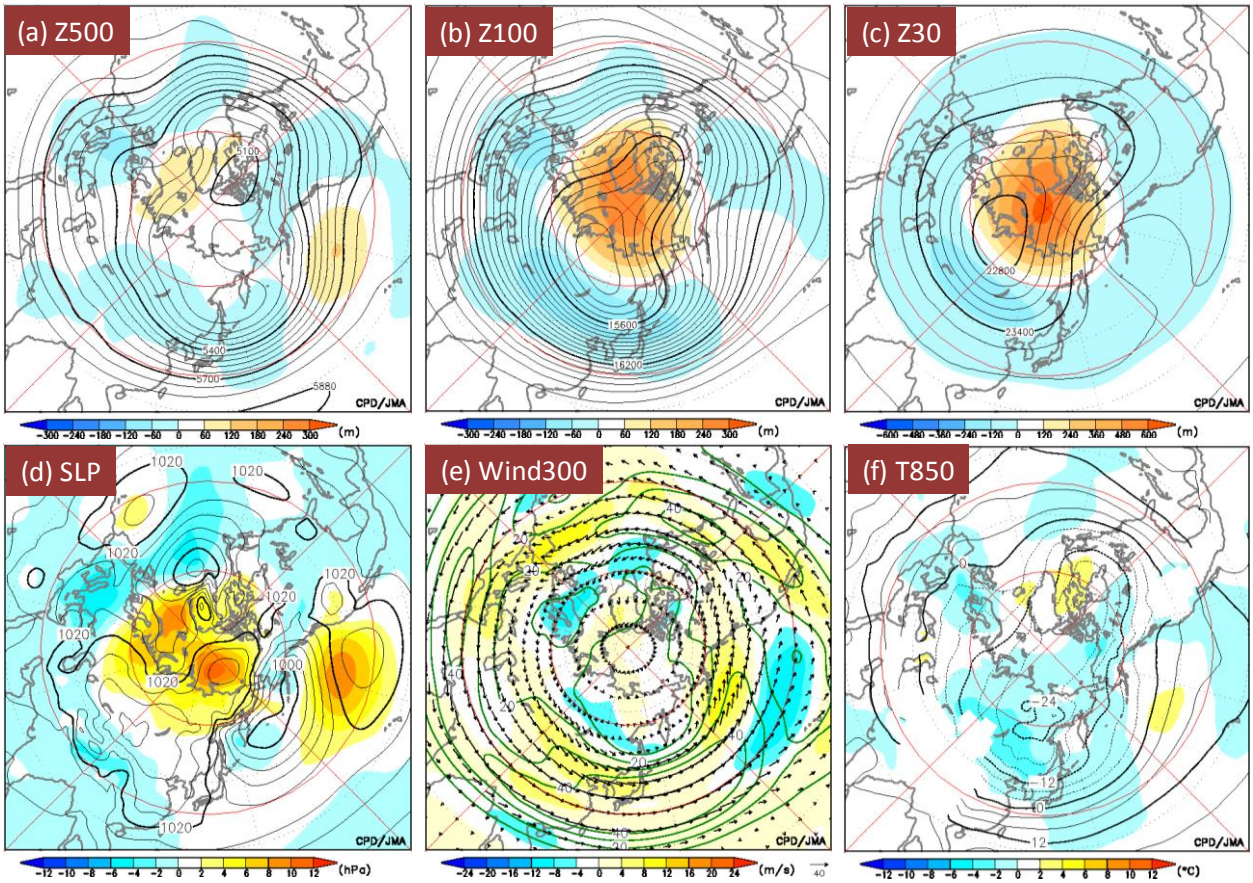

Figure 16 Three-month mean atmospheric circulation in the Northern Hemisphere for December 2012 – February 2013
The contours indicate (a) 500-hPa height, (b) 100-hPa height, (c) 30-hPa height, (d) sea level pressure, (e) 300-hPa wind, and (f) 850-hPa temperature at intervals of 60 m, 60 m, 120 m, 4 hPa, 10 m/s and 4˚C, respectively. The shading indicates related anomalies.

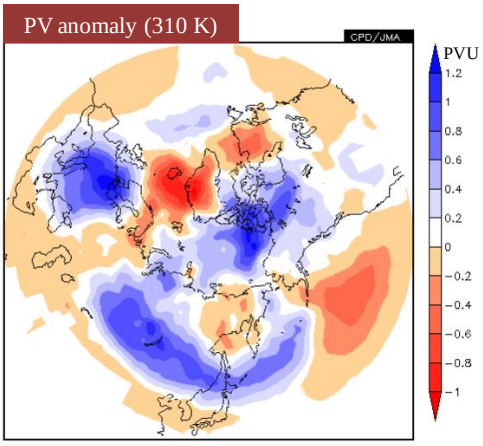

Figure 17 Three-month mean potential vorticity anomalies on the 310-K isentropic surface in the Northern Hemisphere for December 2012 – February 2013

In the stratosphere, the polar vortex remained weak during winter (Figure 18), especially in January 2013 when a major stratospheric sudden warming event occurred (Figure 19). Prevailing planetary wave packets propagated from the troposphere to the stratosphere during December and January (Figure 20 (b)). In association, the polar night jet stream remained weaker than normal during winter (Figure 20 (a)). Easterly wind anomalies in the stratosphere (shown with blue shading in Figure 20 (a)) exhibited peaks with a lag of several days behind the enhancement of upward wave propagation from the troposphere (shown as peaks with red shading in Figure 20 (b)), and easterly anomalies in turn frequently extended from the stratosphere to the troposphere.

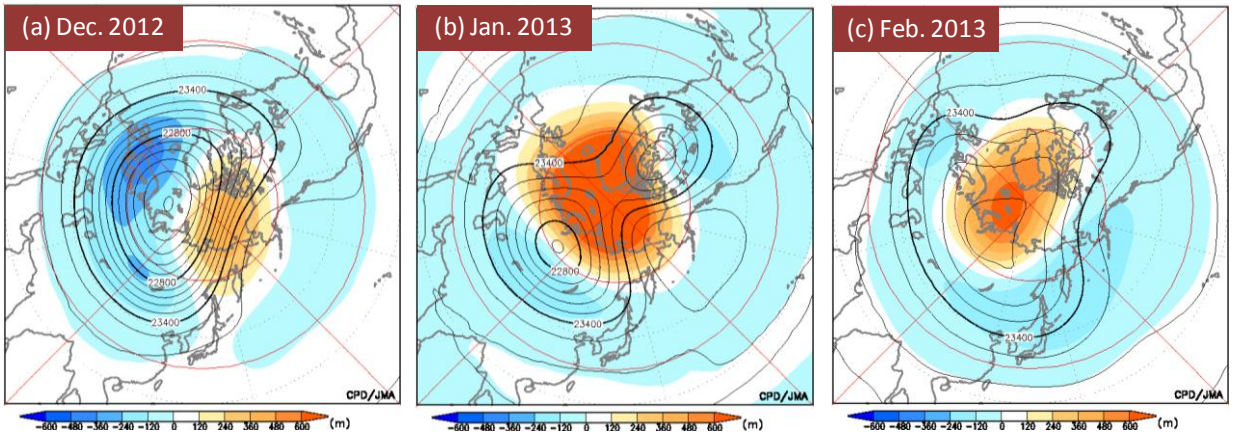

Figure 18 Monthly mean 30-hPa height for (a) December 2012, (b) January 2013 and (c) February 2013
The contours indicate 30-hPa height at intervals of 120 m, and the shading shows related anomalies.

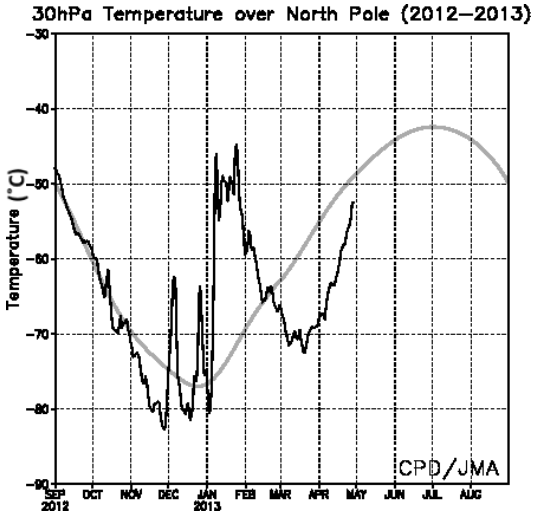

Figure 19 Time-series representation of temperatures at the 30-hPa level over the North Pole (September 2012 – April 2013)
The black line shows daily temperatures, and the gray line indicates the climatological mean.

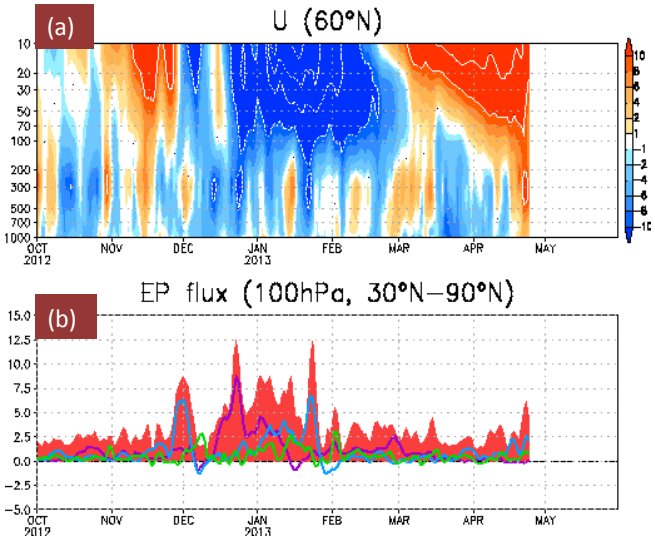

Figure 20 (a) Time-height cross section of zonal mean zonal wind anomalies (m/s) at 60°N, and (b) time-series representation of vertical components of EP flux averaged over 30°N – 90°N at the 100-hPa level (October 2012 – April 2013)
The shading in (a) indicates zonal mean zonal wind anomalies. The red bars in (b) denote the vertical component of EP flux for whole zonal wave numbers. The purple, light-blue and light-green lines denote the vertical components of EP flux for zonal wavenumbers 1, 2 and 3, respectively. The unit for the vertical component of EP flux is m^2/s^2.

3. Primary factors

3.1 Arctic sea ice and high SSTs

During winter 2012/2013, the sea ice extent in the Arctic Ocean remained far below the 1979 – 2000 average, especially in the Barents Sea and the Kara Sea (Figure 21). According to statistical analysis (Figure 22), atmospheric circulation anomalies over Eurasia seen with light sea ice coverage around these seas echoed related anomalies observed during winter (Figure 16), although areas of high sea level pressure with statistical confidence were seen over southern Siberia (Figure 22 (b)) while the anomalies observed were seen over the northern part. Recent studies (e.g., Honda et al. 2009, Inoue et al. 2012) have reported that a reduction in the amount of floating sea ice tends to induce amplification of the Siberian High, leading to cold anomalies in East Asia.

Assessment to determine how SST and sea ice anomalies influence atmospheric circulation was implemented using the atmospheric general circulation model (AGCM) of the Japan Meteorological Agency's one-month prediction model (JMA 2013). The results showed that atmospheric circulation in connection with global SST and sea ice conditions for winter (Figure 23) resembled cold-season conditions (Figure 16) featuring negative AO-like patterns, blocking ridges around eastern Siberia and troughs over northern East Asia. The results of a large ensemble of experiments performed by Deser et al. (2007) using the AGCM showed that high SSTs and light sea ice extents in the North Atlantic sector can force the hemispheric North Atlantic Oscillation-Northern Annular Mode (NAO-NAM) pattern.

Thus, the light sea ice coverage observed around the Barents Sea and the Kara Sea and high SSTs in the Arctic region and the northern North Atlantic may have contributed to the development of negative AO patterns and blocking highs, and consequently the enhancement of the Siberian High.

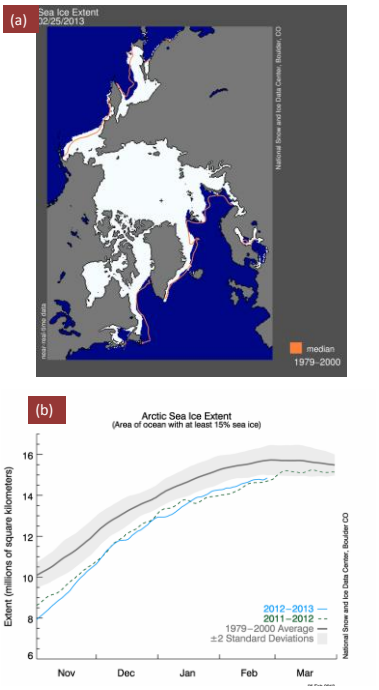

Figure 21 Arctic sea ice extent for winter 2012/2013

(a) Arctic sea ice extent as of 25 February 2013. The orange line shows the 1979 to 2000 median extent for that month, and the black cross marks the geographic North Pole. (b) Daily Arctic sea ice extent as of 25 February 2012, along with the corresponding values for the previous year. The current year is shown in light blue, and 2011 – 2012 is shown in dashed green. The gray area around the average line shows the two-standard-deviation range of the data.

(Sources: National Snow and Ice Data Center (NSIDC), USA, at http://nsidc.org/arcticseaicenews/)

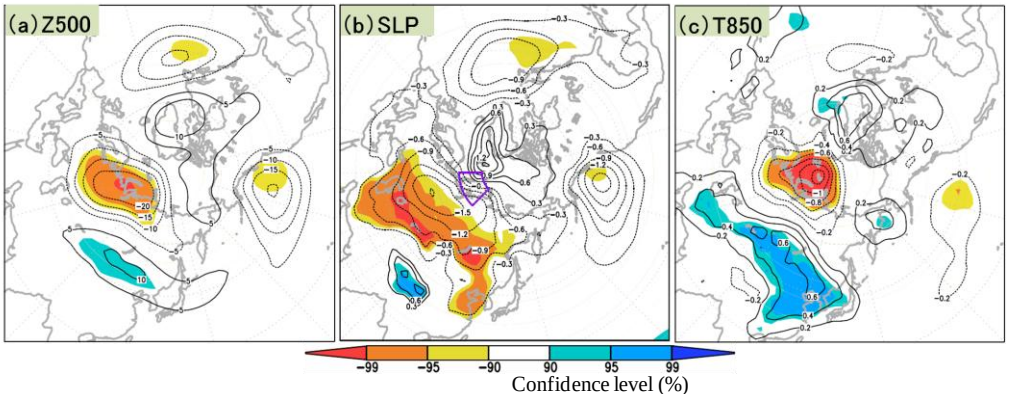

Figure 22 Three-month mean (a) 500-hPa height, (b) sea level pressure, and (c) 850-hPa temperature regressed onto area-averaged sea ice extents around the Barents Sea and the Kara Sea (70˚N – 80˚N, 45˚E – 90˚E) for winters (December – February) from 1979/1980 to 2010/2011

The contour intervals are (a) 5 m, (b) 0.3 hPa, and (c) 0.2˚C. The shading indicates confidence levels as indicated by t-testing. Long-term trends were removed from the datasets before statistical analysis was performed.

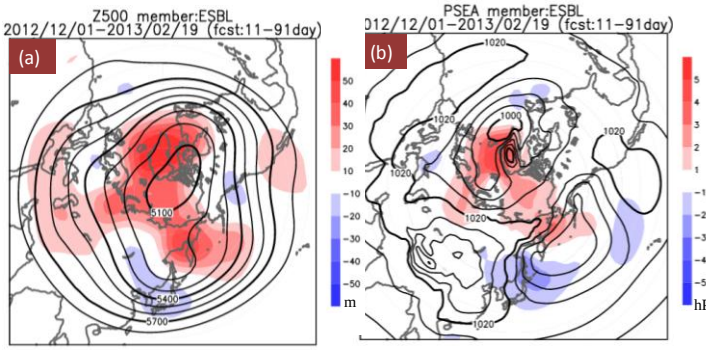

Figure 23 Impacts of sea surface temperature and sea ice anomalies on atmospheric circulation for winter 2012/2013

(a) shows responses of the 500-hPa height to global sea surface temperature (SST) and sea ice anomalies based on output from the Japan Meteorological Agency one-month prediction model (atmospheric general circulation model). In this experiment, 11 members of the model were run and forced with real and normal conditions of daily SST and sea ice. The contours indicate ensemble-mean responses to actual conditions, which are those averaged from 1 December, 2012, to 19 February, 2013. The shading shows deviations between ensemble-mean responses to actual conditions and those to the normal. (b) As per (a), but for sea level pressure at contour intervals of 5 hPa.

3.2 Troposphere-stratosphere interaction

Planetary wave packets of zonal wavenumber 2 propagated upward in the mid-latitudes of the Northern Hemisphere, reflected around the tropopause, turned northward, and converged in the upper troposphere of the high latitudes (Figure 24 (a)). Divergence and convergence of EP flux lead to acceleration and deceleration of westerly winds. As a result, northward wave propagation from mid- to high latitudes contributed to the development of negative AO-like conditions. The path of the wave propagation was consistent with the distribution of the refractive index related to the vertical profile of mean westerly winds (Figure 24 (b)). The vertical profile of westerly winds may have been affected by dominant wave propagation originating in the mid-latitudes.

Thus, it can be hypothesized that interaction between the troposphere and the stratosphere may have contributed to negative AO-like patterns, although further investigation is needed.

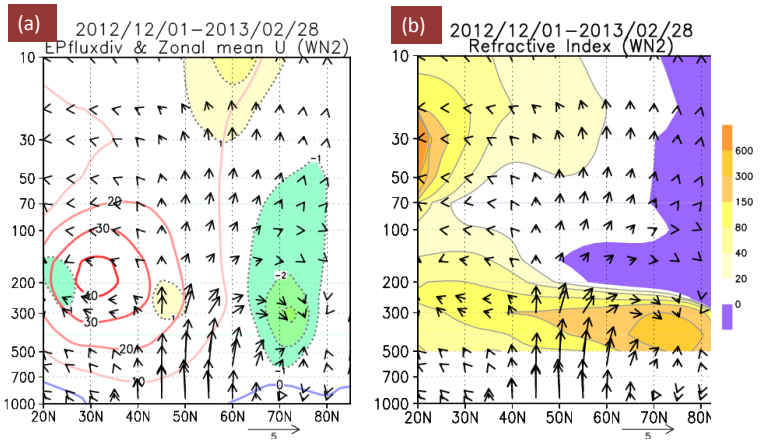

Figure 24 Latitude-height cross section of zonally averaged zonal wind, EP flux and the refractive index for winter 2012/2013

The vectors indicate EP flux for zonal wavenumber 2 in both (a) and (b). (a) The solid contours show zonal wind at intervals of 10 m/s. The shading and dashed contours denote divergence (yellow: positive values) and convergence (negative values) of EP flux at intervals of 1 m/s/day (zero not shown). (b) The shading indicates the refractive index. Wave packets can propagate only in areas with positive index values, and areas with high values act as waveguides.

3.3 Tropical convection and SSTs

The results of AGCM experiments forced with global SST anomalies show upper-level divergence anomalies around the eastern Indian Ocean and anticyclonic and cyclonic circulation anomalies over southern Asia and Japan, respectively (Figure 25). These anomaly patterns resemble those observed for winter (Figure 15). The results of linear baroclinic model experiments forced with convective heating anomalies over the eastern Indian Ocean also show such upper-level circulation anomaly patterns (Figure 26). It can therefore be presumed that enhanced convective activity around the eastern Indian Ocean in association with high SSTs contributed to southward meandering of the jet stream near Japan.

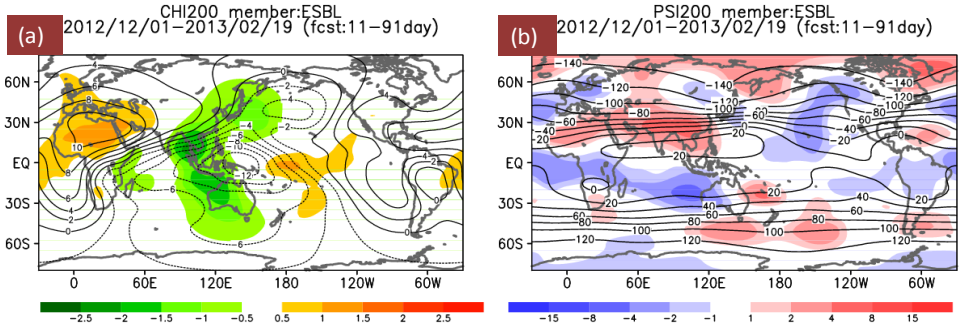

Figure 25 Impacts of sea surface temperature and sea ice anomalies on atmospheric circulation in the upper troposphere for winter 2012/2013

As per 23, but (a) for 200-hPa velocity potential at contour intervals of 2×10^6 m^2/s, and (b) for the 200-hPa stream function at contour intervals of 20×10^6 m^2/s.

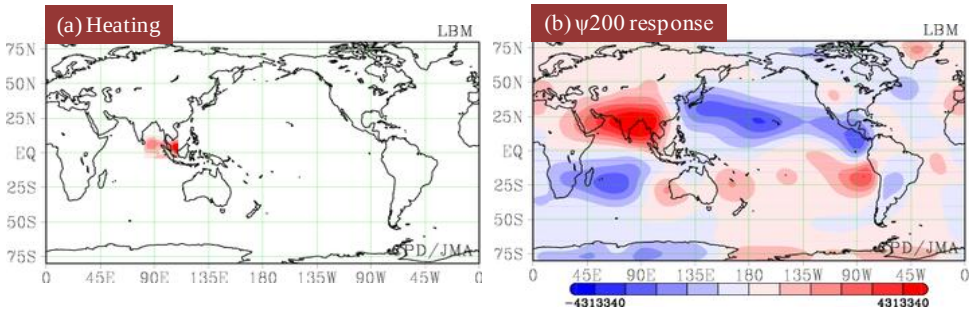

Figure 26 Steady response in a linear baroclinic model (LBM) to heating anomalies around the eastern Indian Ocean for winter 2012/2013

(a) The red shading indicates diabatic heating for the LBM with the basic state for December-January-February (i.e., the 1981 – 2010 average based on JRA-25 data). (b) The shading denotes the steady response of 200-hPa stream function anomalies (m^2/s). These anomalies as responses represent deviations from the basic states, and are additionally subtracted from the zonal averages of the anomalies.

4. Summary

In the 2012/2013 Asian winter monsoon season, northern East Asia experienced a cold winter in association with negative AO-like conditions and blocking patterns around eastern Siberia. The characteristic atmospheric circulation causing the cold conditions may have been related to high SSTs and light sea ice coverage in the Arctic region, troposphere-stratosphere interaction, and enhanced convection around the eastern Indian Ocean. The possible primary factors contributing to these conditions are summarized in Figure 27, but the related mechanisms have not yet been fully clarified.

(1: Kazuyoshi Yoshimatsu; 2 – 4: Shotaro Tanaka, Climate Prediction Division)

References

Deser, C., R. A. Tomas, and S. Peng, 2007: The transient atmospheric circulation response to North Atlantic SST and sea ice anomalies. *J. Climate*, **20**, 4751 – 4767.

Honda, M., J. Inoue, and S. Yamane, 2009: Influence of low Arctic sea-ice minima on anomalously cold Eurasian winters. *Geophys. Res. Lett.*, **36**.

Inoue, J., M. Hori, and K. Takaya, 2012: The Role of Barents Sea Ice in the Wintertime Cyclone Track and Emergence of a Warm-Arctic Cold-Siberian Anomaly. *J. Climate*, **25**, 2561 – 2568.

JMA, 2006: Characteristics of Global Sea Surface Temperature Data (COBE-SST), *Monthly Report on Climate System*, Separated Volume No. **12**.

JMA, 2013: Outline of the operational numerical weather prediction at the Japan Meteorological Agency. *Appendix to WMO Technical Progress Report on the Global Data-processing and Forecasting System and Numerical Weather Prediction Research*.

Onogi, K., J. Tsutsui, H. Koide, M. Sakamoto, S. Kobayashi, H. Hatsushika, T. Matsumoto, N. Yamazaki, H. Kamahori, K. Takahashi, S. Kadokura, K. Wada, K. Kato, R. Oyama, T. Ose, N. Mannoji and R. Taira, 2007: The JRA-25 Reanalysis. *J. Meteorol. Soc. Japan*, **85**, 369 – 432.

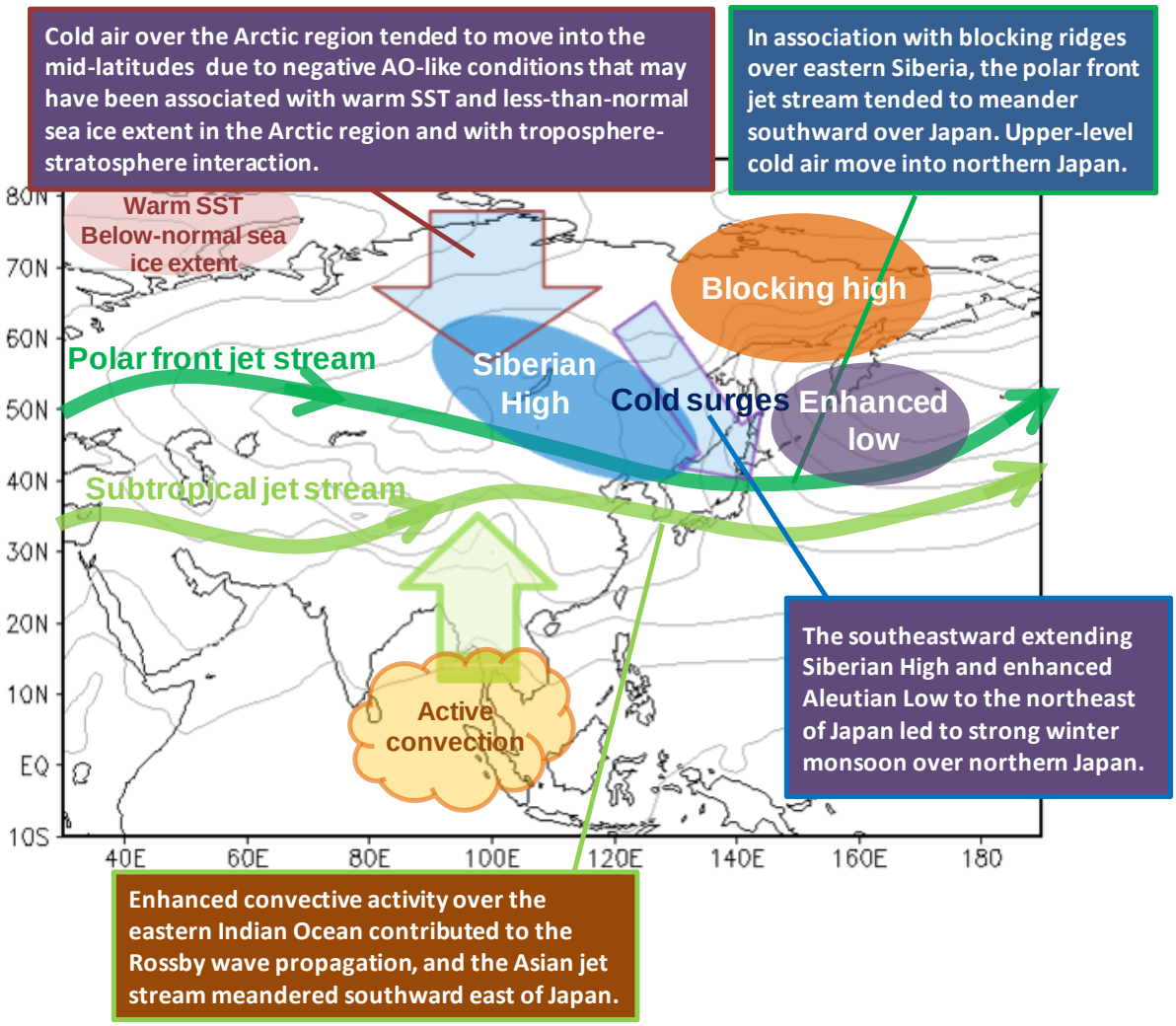

Figure 27 Primary factors contributing to cold winter 2012/2013 in East Asia

Introduction to New Animation Maps Products on the TCC Website

In November 2012, TCC started providing new monitoring products called Animation Maps on its website. These resources are useful in monitoring intraseasonal variations of convective activity and atmospheric circulation. This article briefly introduces the products and highlights some examples of analysis.

Animation Maps are available at http://ds.data.jma.go.jp/tcc/tcc/products/clisys/acmi.html.

1. General explanation

The Animation Maps web pages cover four areas: the Asian Region, the Northern Hemisphere, the Southern Hemisphere and the Global Area. Data on major elements for use in monitoring extratropical circulation (such as sea level pressure, 500-hPa geopotential height and 850-hPa temperature) shown on polar stereographic charts are available on the Northern Hemisphere and Southern Hemisphere pages, and data for use in monitoring tropical convective activity and circulation (such as outgoing longwave radiation (OLR), velocity potential and stream function) are available on the Asian Region and Global Area pages. Animation Maps are available for the period from 1979 to two days prior, and are updated every day.

Figure 28 shows a screenshot of the Northern Hemisphere page with selectable elements and dates in the pull-down menus (B) and (E), respectively. Two elements can be shown simultaneously except on the Global Area page. Daily, 5-day, 7-day, 10-day and 30-day average charts are available for all elements (default: 5-day mean) and can be selected from the pull-down menu (A). Clicking the +1-day and -1-day buttons in (C) moves the charts forward and backward, respectively, by one day. The buttons in D control the animation.

The following sections highlight two examples of analysis using Animation Maps. These involve the propagation of tropical intraseasonal oscillations and the seasonal march of the Asian summer monsoon.

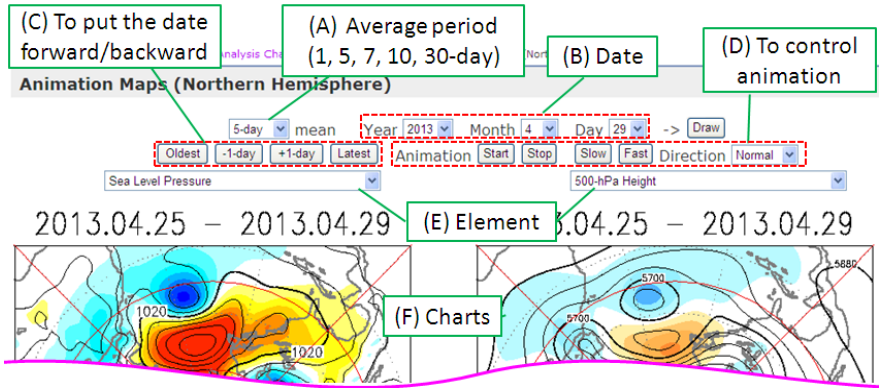

Figure 28 Animation Maps page layout (Northern Hemisphere)

2. Example 1: Propagation of tropical intraseasonal oscillations

The Global Area page supports monitoring of intraseasonal oscillations such as the Madden-Julian Oscillation (MJO), which propagates eastward along the equator. When the pull-down menus here are set as shown in Figure 29, the page displays a seven-day mean chart of OLR (shading), 200-hPa velocity potential (contours) and 200-hPa divergence wind (vectors) anomalies for the period from 24 February to 1 March, 2012. The chart displayed shows blue shading (active convection) and green contours (stronger-than-normal divergence in the upper troposphere) over the Indian Ocean, indicating that the active phase of the MJO is located there.

By clicking the +1-day button repeatedly or the Start button once, the user can follow the eastward movement of the MJO along the equator (Figure 30). It can be seen that the MJO moved eastward and reached the maritime continent in mid-March and the western Pacific late in the month. After that, it was not clearly seen over South America or the Atlantic, but appeared again in amplified form over the Indian Ocean in mid-April.

It is well known that northward-moving intraseasonal oscillations appearing over the northern Indian Ocean during boreal summer affect Asian Monsoon activity. Animation Maps are useful for monitoring such intraseasonal variations.

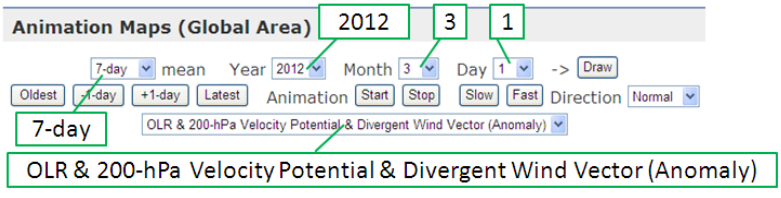

Figure 29 Global Area page pull-down menu settings for Example 1

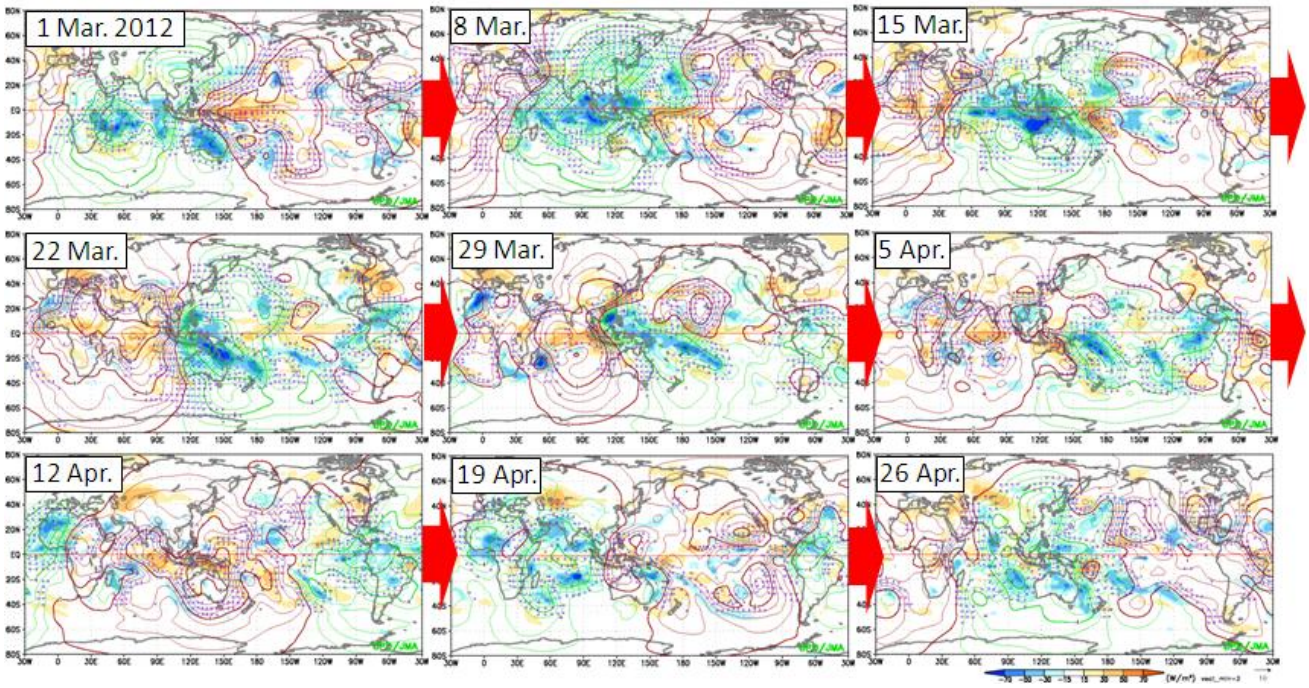

Figure 30 Example of Madden-Julian Oscillation (MJO) monitoring
Each panel shows the seven-day average for the period ending on the date shown in its upper-left corner. The shading indicates outgoing longwave radiation anomalies (OLR; W/m^2), and the contours show 200-hPa velocity potential anomalies at intervals of 1×10^6 m^2/s. The vectors denote 200-hPa divergent wind anomalies.

3. Example 2: Seasonal march of the Asian summer monsoon

This section outlines the display of the Asian summer monsoon's normal seasonal march using Animation Maps from the Asian Region page. Five-day mean charts of normal conditions for upper and lower tropospheric circulation with convective activity can be displayed on this page by setting the pull-down menus as shown in Figure 31. The shading and contours indicate OLR and the stream function, respectively. The panels on the left and right show the upper and lower troposphere.

By clicking the +1-day button repeatedly or the Start button once, the user can follow the seasonal march of the Asian summer monsoon, which exhibits a meridional transition of active convection areas, monsoon westerly winds in the lower troposphere, and the development of the Tibetan High in the upper troposphere (Figure 32).

Running animations of actual and normal conditions side by side on the Asian Region page allows analysis of advances or delays in the seasonal march with respect to the normal.

These examples are only two instances of how Animation Maps can be used. Those on the Northern Hemisphere and Southern Hemisphere pages are useful for monitoring intraseasonal variations of atmospheric circulation such as the development and decay of blocking highs and teleconnection patterns.

(Hiroshi Ohno, Climate Prediction Division)

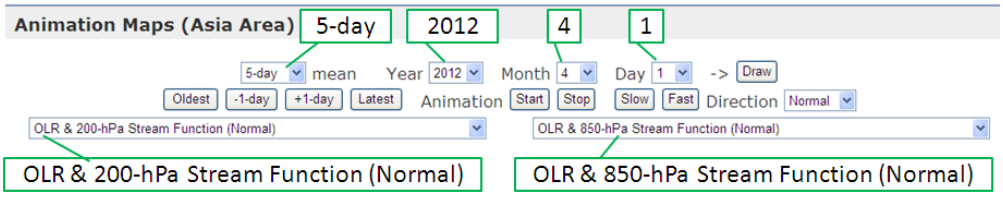

Figure 31 Asian Region page pull-down menu settings for Example 2

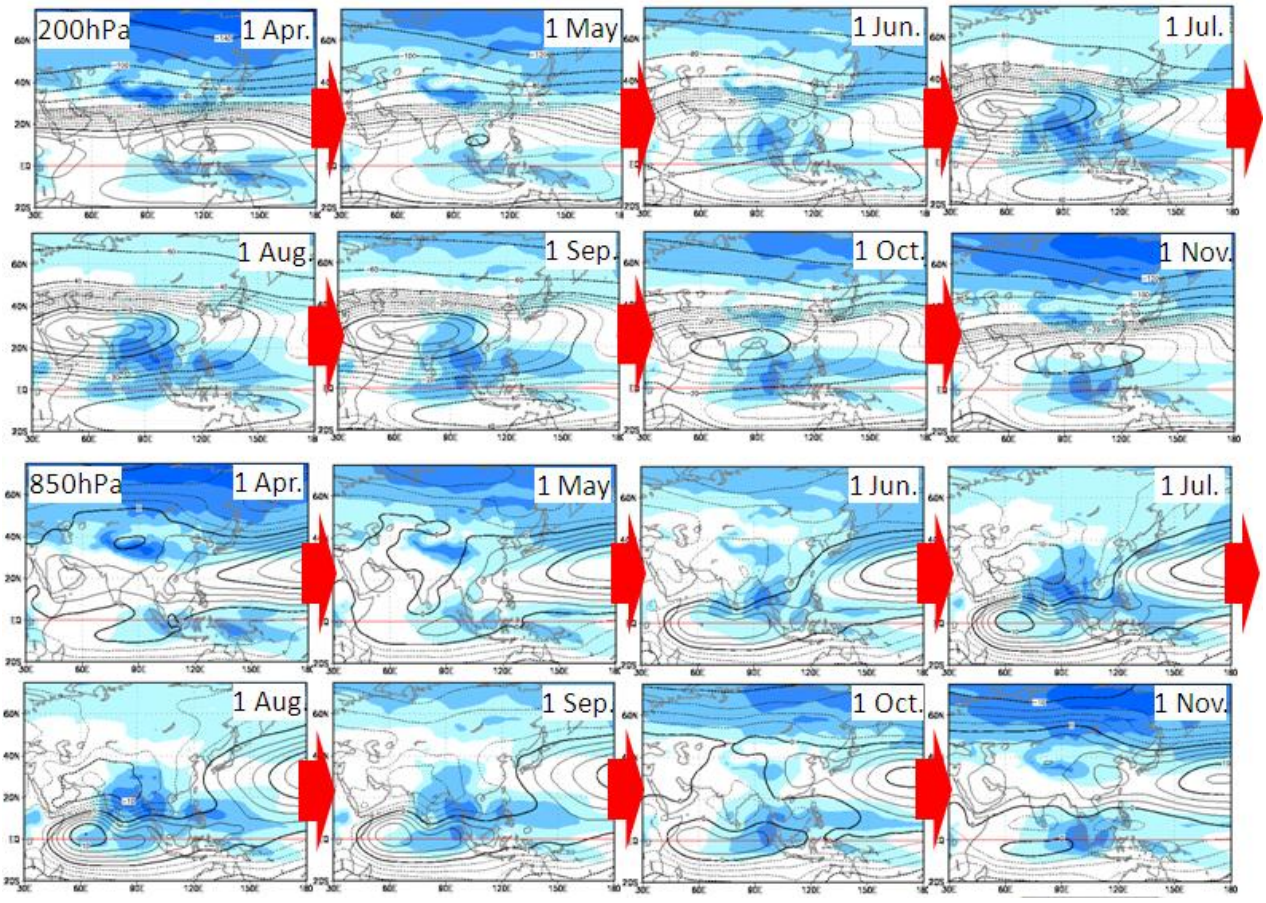

Figure 32 Seasonal march of the normal Asian summer monsoon
Each panel shows the five-day average for the period ending on the date shown in its upper-right corner. The shading indicates normal outgoing longwave radiation (OLR; W/m^2), and the contours show normal (upper) 200-hPa and (lower) 850-hPa stream functions at intervals of 5 and 2.5 x 10^6 m^2/s, respectively.

New design of RA II RCC Portal Site

WMO's two Regional Climate Centers (RCCs) in the Regional Association II (Asia), the Beijing Climate Center (BCC, China) and the Tokyo Climate Center (TCC, Japan) collaboratively developed an RA II RCC portal website in 2007. It provides links to a variety of climate products in line with RCC mandatory functions as well as information on relevant events/meetings/workshops.

In addition to these two Centers, the North Eurasian Climate Centre (NEACC) of the Russian Federation is expected to be formally designated as a new RCC in RA II at the coming 65th session of the WMO Executive Council. In response, BCC and TCC have introduced a new design on the website to add links to climate products provided by NEACC.

Please visit the RA II RCC portal site at http://www.rccra2.org/.

(Ryuji Yamada, Tokyo Climate Center)

Participation of TCC Experts in RCOFs and Expert Visit to BMKG

WMO Regional Climate Outlook Forums (RCOFs) bring together national, regional and international climate experts on an operational basis to produce regional climate outlooks based on input from participating NMHSs, regional institutions, Regional Climate Centers and global producers of climate predictions. By providing a platform for countries with similar climatological characteristics to discuss related matters, these forums ensure consistency in terms of access to and interpretation of climate information.

In April 2013, TCC experts participated in two RCOFs. These were the ninth session of the Forum on Regional Climate Monitoring, Assessment and Prediction for Regional Association II (FOCRAII) held in Beijing, China, from 8 to 10 April, and the fourth session of the South Asian Climate Outlook Forum (SASCOF-4) held in Kathmandu, Nepal, from 18 to 19 April. At both the events, the TCC attendees gave presentations on seasonal predictions based on JMA's numerical model and participated in discussions to produce consensus forecasts.

In addition to contributing to RCOFs, the Center dispatches experts to NMHSs as necessary and/or upon request. In February 2013, TCC experts visited Indonesia's Meteorological, Climatological and Geophysical Agency (BMKG) to provide follow-up on the installation of a module for site-specific probabilistic guidance in one-month forecasting, which will form a part of its Climate Early Warning System (BMKG CEWS). The experts also discussed and exchanged views with BMKG staff members on improving climate services and engaging in possible future cooperation.

(Ryuji Yamada, Tokyo Climate Center)

Pilot Project on Information Sharing on Climate Services

The Global Framework for Climate Service (GFCS) is one of the current top five priorities of WMO. For its successful implementation, it is important to share good practices and lessons learned, including experienced project management capabilities, to develop projects and improve climate services by NMHSs as well as to avoid duplication and minimize the risk of failure.

The WMO Regional Association II, at its fifteenth session (December 2012, Doha, Qatar), decided to establish a pilot project on information sharing on climate services. The project aims at sharing information on climate services and best practices of climate information among NMHSs in the region for the successful implementation of GFCS.

TCC has been designated as Lead for the project to establish and maintain a dedicated web site. To collect relevant information from NMHSs, TCC has developed a questionnaire for the project, which has already been distributed to nominated focal points. Those who have not yet registered focal points, please provide the WMO Secretariat with information on your focal point.

The submitted questionnaire will be organized on the pilot project website, which is expected to be useful for considering future actions required to facilitate the utilization of climate information. The website for the project will be made available in due course.

Your active participation in the pilot project would be greatly appreciated.

(Ryuji Yamada, Tokyo Climate Center)

Any comments or inquiry on this newsletter and/or the TCC website would be much appreciated. Please e-mail to tcc@met.kishou.go.jp.

(Editors: Teruko Manabe, Ryuji Yamada and Kenji Yoshida)

Tokyo Climate Center (TCC), Climate Prediction Division, JMA
Address: 1-3-4 Otemachi, Chiyoda-ku, Tokyo 100-8122, Japan
TCC Website: http://ds.data.jma.go.jp/tcc/tcc/index.html